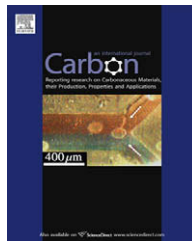




ELSEVIER

available at www.sciencedirect.comjournal homepage: www.elsevier.com/locate/carbon

Improving the adhesion of carbon nanotubes to a substrate using microwave treatment

Huan-Chieh Su ^a, Chang-Hsiao Chen ^b, Yung-Chan Chen ^c, Da-Jeng Yao ^b,
Hsin Chen ^c, Yen-Chung Chang ^d, Tri-Rung Yew ^{a,*}

^a Department of Materials Science and Engineering, National Tsing Hua University (NTHU), 101, Sec. 2, Kuang-Fu Road, Hsinchu 30013, Taiwan

^b Institute of Nano Engineering and Micro System, NTHU, Hsinchu 30013, Taiwan

^c Institute of Electronics Engineering, NTHU, Hsinchu 30013, Taiwan

^d Institute of Molecular Medicine, NTHU, Hsinchu 30013, Taiwan

ARTICLE INFO

Article history:

Received 8 May 2009

Accepted 22 October 2009

Available online xxxx

ABSTRACT

The effect of microwave (MW) treatment to improve the adhesion of carbon nanotubes (CNTs) to a Ni/Ti/Au/SiO₂/Si substrate was examined. CNTs were synthesized at a low temperature (400 °C) by thermal chemical vapor deposition to avoid metal peeling. Results demonstrated that nearly 100% of MW-treated CNTs remained on the substrates even after sonication in a buffer solution. This was a significant improvement of adhesion compared to preparations not undergoing MW treatment, where almost no CNTs remained. Transmission electron microscopy of cross sections showed that before MW treatment, CNTs with Ni nanoparticles were located on the upper part of the Ti underlayer, whereas after MW treatment they were embedded in the Ti underlayer. Based on these results, a mechanism of adhesion improvement by MW treatment is proposed.

© 2009 Elsevier Ltd. All rights reserved.

1. Introduction

Carbon nanotubes (CNTs) have attracted great interest because of their excellent electronic properties [1,2], high thermal conductivity [3], significant mechanical properties [4], and physical and chemical stability [5]. There are many potential applications of CNTs including field-effect transistors (FETs) [6,7], field-emission displays (FEDs) [8,9], bio-sensors [10], atomic force microscopy (AFM) probes [11], and CNT microelectrodes [12,13]. However, the poor adhesion of CNTs onto the substrate becomes a reliability issue and an obstacle for long-term usage of CNT devices. The CNT devices will fail if CNTs are detached from the substrate during operation. This is even more challenging for use of CNT devices in liquid environments, in which the pull and drag of tissues or the flowing of buffer solution may cause detachment of CNTs

from the substrate. The conventional high temperature process of CNT syntheses causes peeling of metal films such as tin, aluminum, and gold, used as underlayers and conducting electrodes. This high temperature process is also incompatible with the complementary metal-oxide-semiconductor (CMOS) interconnect process, which requires a low process temperature (<450 °C). In addition, high temperatures will accelerate detachment of CNTs from their substrate. Therefore, it is critical to both improve the adhesion between CNTs and substrates, and to decrease the temperature at which CNT synthesis occurs to 450 °C or less.

The adhesion of CNTs to the substrate was improved by adding an adhesion layer, such as molybdenum [14], titanium [15] or nickel [16], between the catalyst layer and the substrate. Another approach to provide a strong adhesion of CNTs onto the substrate is thermal deposition of indium

* Corresponding author: Fax: +886 3 5722366.

E-mail address: tryew@mx.nthu.edu.tw (T.-R. Yew).

0008-6223/\$ - see front matter © 2009 Elsevier Ltd. All rights reserved.

doi:10.1016/j.carbon.2009.10.032

and tin metal layers on an indium–tin oxide glass substrate, followed by thermal annealing [17]. An effective method of attaching CNTs to AFM Si tips involving deposition of amorphous carbon has also been reported for AFM applications [18]. In addition, CNT transfer technology is proposed. This is enabled by successful assembly of open-ended structures of CNTs onto substrates by a solder reflow process [19].

This research studies the feasibility of improving CNT adhesion onto substrates utilizing low CNT synthesis temperature (400 °C) and microwave (MW) treatment. A mechanism for CNT adhesion enhancement is proposed.

2. Experimental

The substrates were prepared by deposition of Au, Ti, and Ni onto $\text{SiO}_2/\text{p-Si}$ (resistivity: 5–25 $\Omega \text{ cm}$) wafers sequentially without a break in vacuum of the electron evaporation system. Au was deposited in a 150 nm layer, as a conductor layer for electrical measurement. Ti was deposited with a thickness of 10–20 nm, and is an adhesion layer. A 5 nm layer of Ni serves as a CNT growth catalyst. The 150 nm SiO_2 layer acts as an insulator layer to isolate the upper conductor layer from the bottom Si layer for cyclic voltammetry (CV) measurements. Multi-walled carbon nanotubes (MWCNTs) were then synthesized on the substrate at 400 °C by thermal chemical vapor deposition (CVD). H_2 (10 sccm) was used to prevent oxidation of the catalyst, C_2H_2 (60 sccm) was used as carbon source, and Ar (200 sccm) was used as carrier gas. The process pressure was maintained at 1 Torr.

A commercial MW oven (Panasonic NNS-575 and others) was used to treat the samples (size: 0.5 cm \times 0.5 cm) with as-grown CNTs. The samples were put in the center of the MW oven with a turntable for sample rotation to provide uniform MW absorption in air. The MW powers were set at 200, 400, 900, or 1100 W for a duration of 0.5, 1, 2, 3, or 5 min for process optimization. The MW was used for treatment because it has been reported that MW absorption of CNTs with encapsulated magnetic nanoparticles is more effective at a frequency of about 2.45 GHz [20–22].

To explore the adhesion strength of the CNTs onto the substrate, CNT samples with various MW treatments were immersed into a buffer solution for sonication. The CNT morphology was firstly examined by scanning electron microscopy (SEM, JEOL 6500 and 7000) imaging at a low magnification, in which a uniform CNT density was observed. The CNT numbers were then roughly calculated based on high-resolution top-view and cross-section SEM images that can identify a single CNT clearly, a method similar to those reported by other papers [23,24]. In this work, the CNT number was calculated from a fixed area ($\sim 1 \mu\text{m}^2$) of a top-view SEM image taken at a high magnification. To quantify the CNT number of the samples before and after sonication, three data points for each sample were measured from three different locations of top-view SEM images. The average CNT numbers and their standard deviations for each sample were also calculated. In addition, the CNT number and CNT-to-CNT spacing were further examined and verified based on high-resolution cross-section SEM image. The percentage of as-grown CNTs before sonication was set as 100%. The percent-

ages of CNTs remaining were defined as the ratio of the number of CNTs remaining after various MW treatments and 5 min sonication to that of as-grown CNTs prior to sonication. For example, if the number of as-grown CNTs is 400 in the $1 \mu\text{m}^2$ boxed area, and the number of CNTs after sonication is 200, then the percentage of CNTs remaining is 50%. The adhesion strength of CNTs onto the substrate was based on the percentage of CNTs remaining after sonication. More CNTs remaining means better adhesion of CNTs onto the substrate.

Transmission electron microscopy (TEM, JEOL JEM 2010 and JSM 2100F) was utilized to analyze CNT nanostructure. Cross-section TEM was utilized to analyze the interaction between CNTs, Ni nanoparticles, and the Ti underlayer before and after MW treatment. The energy dispersion spectrum (EDS) line-scanning function in cross-section TEM was used to examine the distribution of elements in the scanned area. Combining cross-section TEM and EDS line-scan, the nanostructure and element distribution could be characterized *in situ*. This enables study of the interaction between CNTs and the substrate, as well as the mechanism of adhesion improvement of CNTs to the substrate.

Micro-Raman spectra (HORIBA JOBIN YVON, HR-800, laser excitation wavelength: 633 nm) were also used to measure the degree of graphitization for CNTs. The D-band intensity is defect-induced (1350 cm^{-1}) and the G-band intensity is a graphite-related optical mode ($1550\text{--}1605 \text{ cm}^{-1}$) [25]. The G-band to D-band intensity ratio (I_G/I_D , G/D ratio) corresponds to the graphitization of CNTs, which can be used as an indication of the CNT quality. A higher I_G/I_D ratio means better graphitization of CNTs. A lower I_G/I_D ratio indicates more defects and amorphous carbon in CNTs [26].

Electrical properties of as-grown CNTs and MW-treated CNTs, in phosphate buffered saline (PBS) solution, were also measured by CV (CH instruments, Model 680 Amp Booster) for future biological applications. The CV experiments were carried out in a three electrode configuration. The Pt coil was used as the counter electrode, Ag/AgCl as the reference electrode, and the CNT electrode as the working electrode. In the CV measurement, the potential was set at -0.4 to 0.6 V to avoid electrolysis of PBS solution. The sweeping rate was 500 mV s^{-1} .

In addition to sonication in buffer solution, another adhesion test was also conducted by inserting the CNT samples into agar gel (quasi-neuron tissue) and dragging them back and forth for 20 times, which was to mimic the puncture of neurons.

3. Results and discussion

The strength of CNT adhesion before and after MW treatments was tested by sonication in a buffer solution. The SEM images of as-grown CNTs without sonication in Fig. 1a show that CNTs were synthesized at 400 °C, 1 Torr with a C_2H_2 to H_2 flow ratio of 6 (60 sccm/10 sccm). Fig. 1b shows the high-resolution TEM image of the CNTs removed by sonication and confirms that the CNTs grown are MWCNTs. However, the percentage of CNTs remaining for the samples without MW treatment decreases dramati-

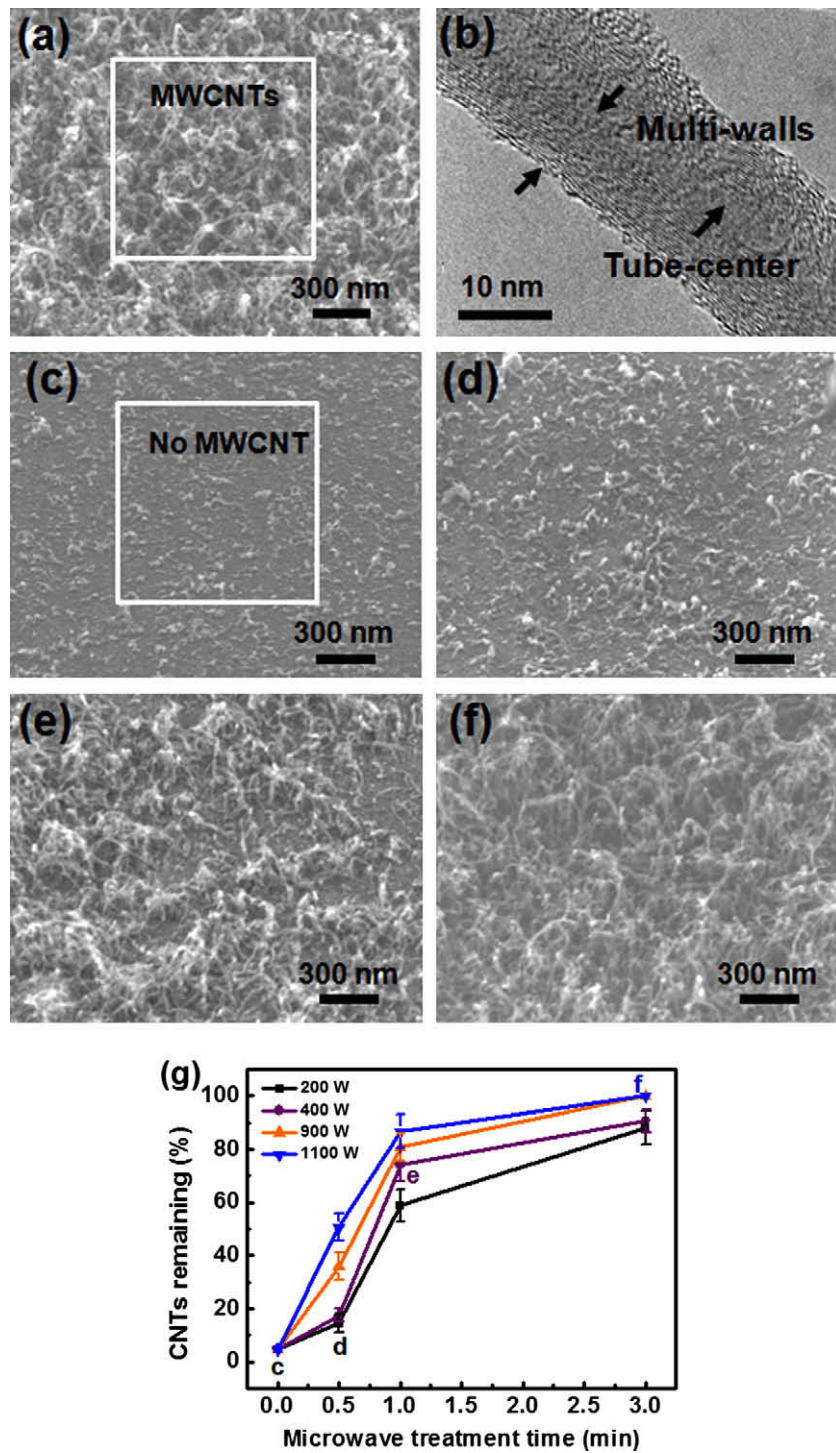


Fig. 1 – (a) Top-view SEM image of as-grown CNTs without sonication, with (b) the high-resolution TEM image showing the CNT grown is a multi-walled CNT. Top-view SEM images of (c) as-grown CNTs after 5 min sonication, and the samples with MW treatment at (d) 200 W, 0.5 min, (e) 400 W, 1 min, and (f) 1100 W, 3 min, after 5 min sonication. (g) The trend charts show the percentages of CNTs remaining after 5 min sonication versus MW treatment time at various powers with the data points of c, d, e and f corresponding to figures c–f, respectively. The $1 \mu\text{m}^2$ boxed area in (a) and (c) was used to count the CNT number and calculate CNTs remaining.

cally with the duration of sonication, i.e., about 90%, 75%, 40%, and 5% after 0.5, 1, 2, and 5 min sonication, respectively. As shown in Fig. 1c, as-grown CNTs were almost completely removed after 5 min sonication. It indicates

that the adhesion of as-grown CNTs onto the substrate is weak even with a Ti adhesion layer. This becomes a reliability issue and an obstacle for long-term usage of CNT devices.

To improve CNT adhesion onto substrates, MW treatment was proposed in this work and a series of experiments were conducted by varying MW process parameters. Fig. 1d-f shows the SEM images after 5 min sonication for the samples pre-treated with different MW parameters including (d) 200 W, 0.5 min, (e) 400 W, 1 min, (f) 1100 W, 3 min, respectively. The trend charts in Fig. 1g show the percentages of CNTs remaining after 5 min sonication versus MW treatment time at various powers with the data points of c, d, e and f corresponding to Fig. 1c-f, respectively. It can be observed that the percentage of CNTs remaining increases with the MW treatment time and power. Moreover, the percentage of CNTs remaining reaches almost 100% after MW treatment for 3 min at a MW power of 900 W or higher. This shows that MW treatment is an effective method to improve the adhesion of CNTs onto the substrate. The difference in percentage of CNTs remaining can be clearly observed and the effect of MW treatment is demonstrated.

Raman spectra were used to characterize the graphitization of as-grown CNTs, as well as those after MW treatment for 0.5, 1, 2, 3 and 5 min at 900 W, as shown in Fig. 2a. The impact of graphitization due to MW treatment can be observed. Fig. 2b shows the G/D ratio, I_G/I_D , of the Raman spectra versus MW treatment time at 900 W. I_G/I_D for as-grown CNTs is 0.42. The ratio decreased slightly as the MW treatment time increased from 0.5 min ($I_G/I_D = 0.41$) to 5 min ($I_G/I_D = 0.33$). The lower I_G/I_D ratio indicates a lower degree of graphitization for MW-treated CNTs. These results reveal that the graphitization of CNTs was slightly damaged after MW treatment. This indicates that MW treatment may lead to slight degradation of CNT device performance.

Electrical properties of as-grown CNTs and MW-treated CNTs in PBS solution were compared to investigate the impact of MW treatment. Fig. 3 shows the CV data of as-grown and MW-treated CNTs in PBS solution at a scan rate (v) of 500 mV s⁻¹. The capacitance (C) was derived according to the following equation [27], $C = \Delta i/2v$ where Δi is the current charge deviation between positive and negative voltage scan. The capacitance was calculated to be 5.13 mF cm⁻² for as-grown CNTs, and 4.86, 5.29, and 4.15 mF cm⁻² for the CNTs with MW treatment for 3 min at 400 W, 1 min at 1100 W, and 3 min at 1100 W, respectively. The capacitances for MW-treated CNTs decreased slightly compared with that of as-grown CNTs. In addition, a capacitance of about 33 μ F cm⁻² for the

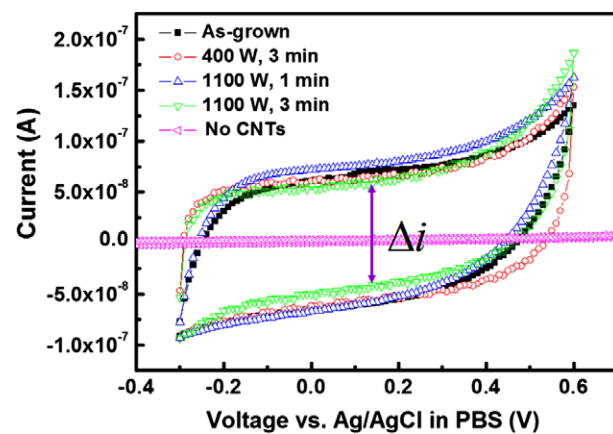


Fig. 3 – CV of as-grown CNTs and MW-treated CNTs in PBS solution. The scan rate was 500 mV s⁻¹.

electrode without CNTs is about 100 times smaller than those with CNTs. Because the capacitance corresponds to CNT-PBS interface properties, it can be speculated that CNTs were only slightly damaged by MW treatment. The results of CV are consistent with those of the Raman spectra.

In order to understand the mechanism of adhesion improvement of CNTs onto the substrate by MW treatment, cross-section TEM and EDS line-scans were used to inspect the nanostructure of the CNTs/Ni/Ti multilayer stack before and after MW treatment, as shown in Fig. 4. It can be observed that CNT growth employs the “base growth” mechanism [28], with Ni remaining in the bottom of the CNT. Ni nanoparticles were encapsulated within CNTs grown from the upper part of the Ti underlayer and were identified as nickel carbide by a diffraction pattern (DP) in TEM, as shown in Fig. 4a. After MW treatment, it can be observed that the major difference between Fig. 4a and c is that the Ni nanoparticle was embedded in the Ti underlayer. EDS line-scans of Fig. 4b and d were performed in cross-section TEM for the same areas of the samples as those taken in Fig. 4a and c, respectively. These show the distribution of elements in the scanned area and confirm the shift of the Ni peak into the Ti matrix after MW treatment (Fig. 4d) versus before treatment (Fig. 4c). These results indicate that the Ni nanoparticles are distributed near the upper surface of Ti underlayer before MW treatment,

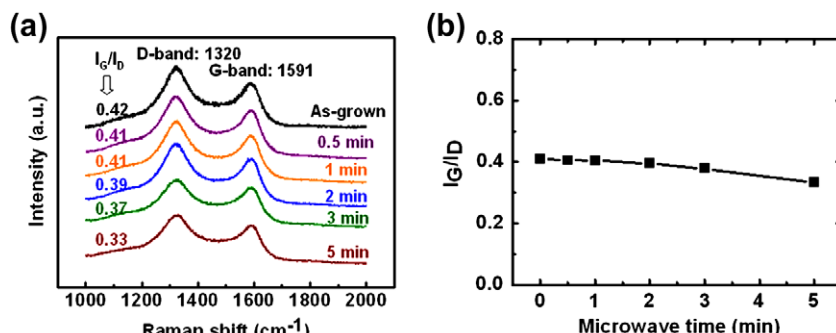


Fig. 2 – (a) The Raman spectra of as-grown CNTs versus CNTs after MW treatment for 0.5, 1, 2, 3 and 5 min at 900 W, and (b) the trend chart of G/D ratio (I_G/I_D) versus MW treatment time.

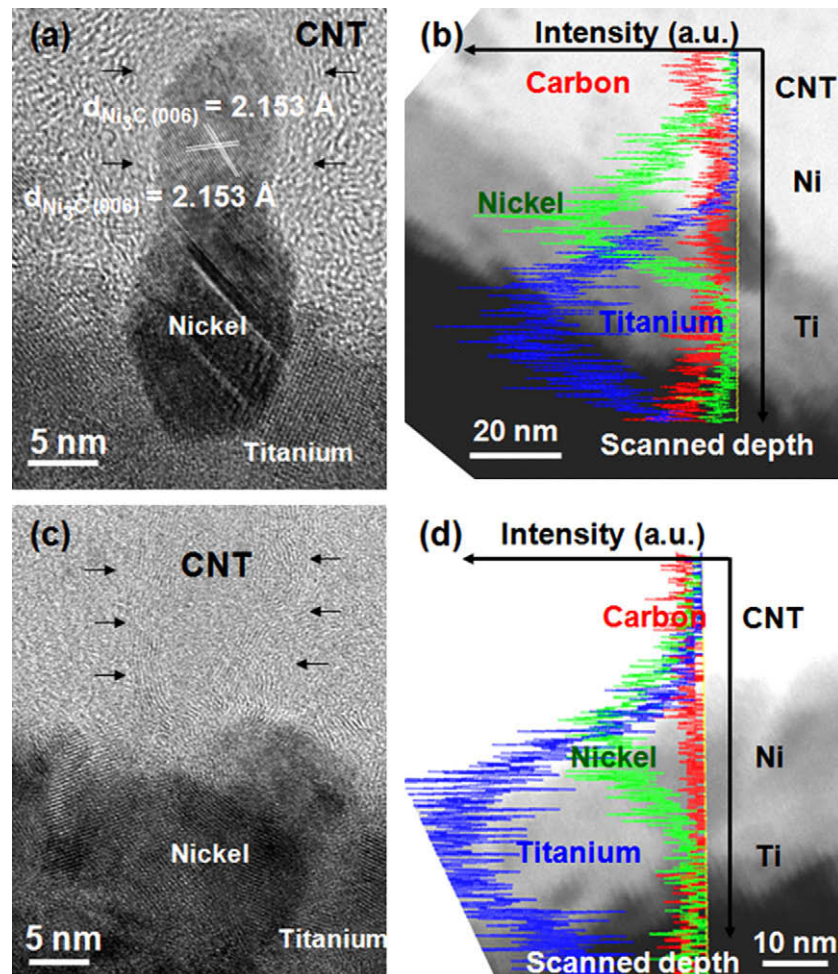


Fig. 4 – The (a) cross-section TEM images and (b) EDS line-scan for a CNTs/Ni/Ti multilayer stack to show catalyst distribution. (c) and (d) show those after MW treatment, respectively.

and are distributed near the inner part of Ti underlayer after MW treatment.

The effectiveness of adhesion improvement of CNTs onto substrates is most likely related to the absorption of MW energy by CNTs/Ni/Ti/Au materials on SiO_2/Si . MW treatment can be used not only for annealing, but also for heating materials rapidly and selectively. The good MW absorption of CNTs is attributed to their large dielectric loss [29]. Furthermore, CNTs with magnetic Fe and Ni nanoparticles exhibit excellent MW absorption properties, which were attributed to their dielectric properties and high magnetic loss, as reported in [30–32]. The embedding of Ni nanoparticles and CNTs into a Ti matrix improves the adhesion of CNTs onto the substrate. One possible reason for this is that MW treatment provides an annealing effect as the CNTs/Ni/Ti multilayer stack absorbs MW energy. The same results were obtained for the MW treatment on the CNTs with a Fe catalyst. Using magnetic nanoparticles as catalysts works for CNT depositions, because the magnetic nanoparticles encapsulated within the CNTs are outstanding MW absorption materials. These materials can therefore be annealed effectively by MW treatment. In this work, different brands of commercial MW ovens were used to carry out the MW

treatment process and showed the same results. Furthermore, the adhesion enhancement of CNTs was also observed using glass substrates. It is speculated that this approach is suitable for other substrates (such as SiO_2 , sodalime glass, and Teflon polycarbonate substrates) because the MW absorption is achieved mainly by CNTs/Ni and is less dependent on the substrate [20].

Based on these results, we propose a model for the adhesion improvement of CNTs onto the substrate by MW treatment, as shown in Fig. 5. The diagrams in Fig. 5a and b show the as-grown CNTs and their transformation after MW treatment, respectively. The Ni nanoparticles for as-grown CNTs were located near the upper surface of the Ti underlayer prior to MW treatment. The nanoparticles become embedded in the Ti underlayer during MW treatment. This implies a strong interaction of Ni, Ti and CNTs [33], as shown in Fig. 4, as well as the formation of strong bonding between Ni nanoparticles and the Ti underlayer during CNT growth and the MW treatment process [15]. This improves the adhesion of CNTs onto the substrate.

In addition to sonication in buffer solution, another adhesion test was also conducted by inserting the CNT samples

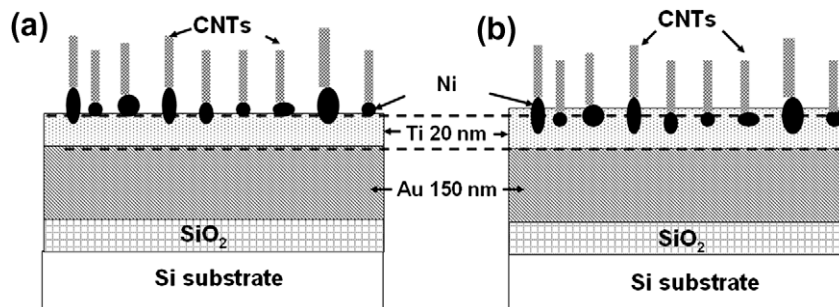


Fig. 5 – Diagrams showing (a) as-grown CNTs and (b) CNTs after MW treatment on Ni/Ti substrates.

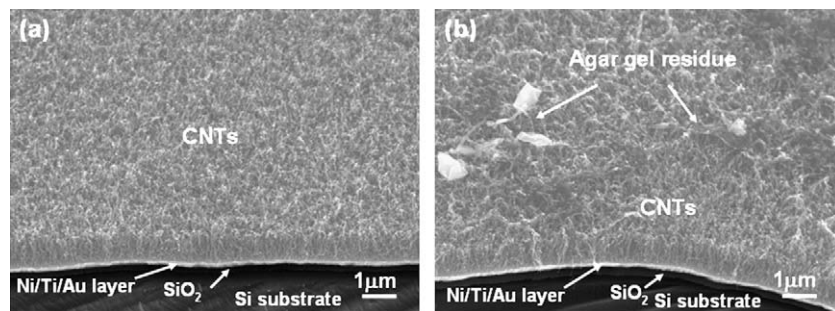


Fig. 6 – Cross-section SEM images show the CNTs on Ni (5 nm)/Ti (20 nm)/Au/SiO₂/Si substrates (a) before and (b) after insertion and dragging them back and forth in agar gel for 20 times.

into agar gel (quasi-neuron tissue) and dragging them back and forth for 20 times, which was to mimic the puncture of neurons. Fig. 6a and b show the cross-section SEM images of CNTs on substrates before and after insertion, respectively. The CNTs were grown at 400 °C and MW treated at 1100 W for 3 min. As shown in Fig. 6b, the CNTs were not degraded after insertion and dragging them back and forth in agar gel for 20 times.

Biocompatibility is an important criterion for biological applications. For CNTs grown on a Ni/Ti/Au substrate, there are reports that Ni is cytotoxic, releasing harmful Ni ions and causing cell death [34]. However, the thickness of Ni used as a catalyst for CNT growth is several nanometers. This layer becomes nanoparticles encapsulated by CNTs after thermal CVD. In addition, the mechanism of CNT growth employs the “base growth” mechanism with the Ni nanoparticles under dense CNTs. Release of Ni ions from the bottom layer to cells will be reduced. Despite previous reports about the toxicity of Ni, several groups have demonstrated the high viability of a cell culture on as-grown CNTs using Ni as a catalyst [13,35]. Furthermore, a Ti layer was added with the Ni layer to form a Ni-Ti alloy, which has good biocompatibility [36,37]. Some reports show that carbon plasma immersion ion implantation into the Ni-Ti alloy can improve the corrosion resistance and block out-diffusion of Ni. This is similar to the CNTs grown from the catalyst due to carbon diffusion to the nanoparticles [38]. Based on the above reasons, the CNT electrodes with Ni/Ti/Au substrates may be usable for biological applications, such as implanted neural probes. Additionally, the CNT electrodes developed in this work could

be applied to potential applications with less concern about toxicity, such as FEDs and interconnects.

4. Conclusions

We have synthesized CNTs at 400 °C by thermal CVD which is compatible with CMOS process, and have proposed a novel MW-assisted method to improve the adhesion of CNTs onto the substrates. The Ti adhesion layer was deposited between the Ni catalyst and the substrate. The CNT adhesion improved with increase of the Ti thickness. The percentage of CNTs remaining after 5 min of sonication in buffer solution for samples with various MW treatments was compared to that of as-grown CNTs. This was used to examine the adhesion strength. Results revealed that the percentage of CNTs remaining after 5 min of sonication reached nearly 100% for samples with the MW treatment of 3 min at a MW power of 900 W or higher. The Raman spectrum showed that the CNTs after MW treatment were slightly damaged. CV data showed that CNT electrodes still exhibit high specific capacitance after MW treatment. The proposed mechanism of CNT adhesion improvement by MW treatment is most likely successful due to CNTs with Ni nanoparticles becoming embedded in a Ti matrix after MW treatment. The embedding was possible because of the MW energy absorption of CNTs/Ni/Ti. The above results demonstrate the potential applications of CNT electrodes fabricated in this work, including implanted neural probes, FEDs, and interconnects. These applications are made possible due to the improvement of CNT adhesion for long-term usage and reliability.

Acknowledgments

The authors acknowledge the financial support of the National Science Council under project number NSC97-2627-E-007-002. The authors also would like to thank Prof. H. Chen in the department of Electrical Engineering for the CV measurements and the CNMM for facility supports, as well as very helpful discussions with group members at the Department of Materials Science and Engineering, National Tsing-Hua University.

REFERENCES

[1] Durkop T, Getty SA, Cobas E, Fuhrer MS. Extraordinary mobility in semiconducting carbon nanotubes. *Nano Lett* 2004;4(1):35–9.

[2] Yao Z, Kane CL, Dekker C. High-field electrical transport in single-wall carbon nanotubes. *Phys Rev Lett* 2000;84(13):2941–4.

[3] Hone J, Whitney M, Zettl A. Thermal conductivity of single-walled carbon nanotubes. *Syn Metals* 1999;103:2498–9.

[4] Dresselhaus MS, Dresselhaus G, Eklund PC. *Science of fullerenes and carbon nanotubes*. New York: Academic; 1996. p. 765–802.

[5] Bonard JM, Salvetat JP, Stockli T, de Heer WA, Forro L, Chatelain A. Field emission from single-wall carbon nanotube films. *Appl Phys Lett* 1998;73(7):918–20.

[6] Tans SJ, Verschueren ARM, Dekker C. Room-temperature transistor based on a single carbon nanotube. *Nature* 1998;393(6680):49–52.

[7] Martel R, Schmidt T, Shea HR, Hertel T, Avouris P. Single- and multi-wall carbon nanotube field-effect transistors. *Appl Phys Lett* 1998;73(17):2447–9.

[8] Lim SC, Choi LC, Jeong HJ, Shin YM, An KH, Bae DJ, et al. Effect of gas exposure on field emission properties of carbon nanotube arrays. *Adv Mater* 2001;13(20):1563–7.

[9] Wang QH, Setlur AA, Lauherhaas JM, Dai JY, Seelig EW, Chang RPH. A nanotube-based field-emission flat panel display. *Appl Phys Lett* 1998;72(22):2912–3.

[10] Besteman K, Lee JO, Wiertz FGM, Heering HA, Dekker C. Enzyme-coated carbon nanotubes as single-molecule biosensors. *Nano Lett* 2003;3(6):727–30.

[11] Dai HJ, Hafner JH, Rinzler AG, Colbert DT, Smalley RE. Nanotubes as nanoprobes in scanning probe microscopy. *Nature* 1996;384(6605):147–50.

[12] Wang K, Fishman HA, Dai HJ, Harris JS. Neural stimulation with a carbon nanotube microelectrode array. *Nano Lett* 2006;6(9):2043–8.

[13] Gabay T, Ben-David M, Kalifa I, Sorkin R, Abrams ZR, Ben-Jacob E, et al. Electro-chemical and biological properties of carbon nanotube based multi-electrode arrays. *Nanotechnology* 2007;18(3):035201-1–6.

[14] Zhao Y, Tong T, Delzeit L, Kashani A, Meyyappan M, Majumdar A. Interfacial energy and strength of multiwalled-carbon-nanotube-based dry adhesive. *J Vac Sci Technol B* 2006;24(1):331–5.

[15] Ominami Y, Ngo Q, Suzuki M, Austin AJ, Yang CY, Cassell AM, et al. Interface characteristics of vertically aligned carbon nanofibers for interconnect applications. *Appl Phys Lett* 2006;89(26):263114–6.

[16] Chen ZX, Zhang Q, Lan PX, Zhu BJ, Yu T, Cao GC, et al. Ultrahigh-current field emission from sandwich-grown well-aligned uniform multi-walled carbon nanotube arrays with high adherence strength. *Nanotechnology* 2007;18(26):265702-1–6.

[17] Lim SC, Choi HK, Jeong HJ, Song YI, Kim GY, Jung KT, et al. A strategy for forming robust adhesion with the substrate in a carbon-nanotube field-emission array. *Carbon* 2006;44(13):2809–15.

[18] Nishijima H, Kamo S, Akita S, Nakayama Y, Hohmura KI, Yoshimura SH, et al. Carbon-nanotube tips for scanning probe microscopy: Preparation by a controlled process and observation of deoxyribonucleic acid. *Appl Phys Lett* 1999;74(26):4061–3.

[19] Zhu LB, Sun YY, Hess DW, Wong CP. Well-aligned open-ended carbon nanotube architectures: an approach for device assembly. *Nano Lett* 2006;6(2):243–7.

[20] Hong EH, Lee KH, Oh SH, Park CG. In-situ synthesis of carbon nanotubes on organic polymer substrates at atmospheric pressure. *Adv Mater* 2002;14(9):676–9.

[21] Wadhawan A, Garrett D, Perez JM. Nanoparticle-assisted microwave absorption by single-wall carbon nanotubes. *Appl Phys Lett* 2003;83(13):2683–5.

[22] Wang Y, Iqbal Z, Mitra S. Microwave-induced rapid chemical functionalization of single-walled carbon nanotubes. *Carbon* 2005;43(5):1015–20.

[23] Ren ZF, Huang ZP, Xu JW, Wang JH, Bush P, Siegal MP, et al. Synthesis of large arrays of well-aligned carbon nanotubes on glass. *Science* 1998;282(6):1105–7.

[24] Okita A, Suda Y, Oda A, Nakamura J, Ozeki A, Bhattacharyya K, et al. Effects of hydrogen on carbon nanotube formation in CH_4/H_2 plasmas. *Carbon* 2007;45(7):1518–26.

[25] Dresselhaus MS, Dresselhaus G, Jorio A, Souza Filho AG, Saito R. Raman spectroscopy on isolated single wall carbon nanotubes. *Carbon* 2002;40:2043–61.

[26] Endo M, Kim YA, Fukai Y, Hayashi T, Terrones M, Terrones H, et al. Comparison study of semi-crystalline and highly crystalline multiwalled carbon nanotubes. *Appl Phys Lett* 2001;79(10):1531–3.

[27] Nguyen-Vu TDB, Chen H, Cassell AM, Andrews R, Meyyappan M, Li J. Vertically aligned carbon nanofiber arrays: an advance toward electrical–neural interfaces. *Small* 2006;2(1):89–94.

[28] Baker RTK, Harris PS. *Chemistry and physics of carbon*, vol. 14. New York: Marcel Dekker; 1978. p. 83–165.

[29] Deng LJ, Han MG. Microwave absorbing performances of multiwalled carbon nanotube composites with negative permeability. *Appl Phys Lett* 2007;91(2):023119–21.

[30] Che RC, Peng LM, Duan XF, Chen Q, Liang XL. Microwave absorption enhancement and complex permittivity and permeability of Fe encapsulated within carbon nanotubes. *Adv Mater* 2004;16(5):401–5.

[31] Zhang XF, Dong XL, Huang H, Liu YY, Wang WN, Zhu XG, et al. Microwave absorption properties of the carbon-coated nickel nanocapsules. *Appl Phys Lett* 2006;89(5):053115–7.

[32] Wen F, Yi H, Qiao L, Zheng H, Zhou D, Li F. Analyses on double resonance behavior in microwave magnetic permeability of multiwalled carbon nanotube composites containing Ni catalyst. *Appl Phys Lett* 2008;92(4):042507–9.

[33] Zhang Y, Franklin NW, Chen RJ, Dai HJ. Metal coating on suspended carbon nanotubes and its implication to metal–tube interaction. *Chem Phys Lett* 2000;33(1):35–41.

[34] Funakoshi T, Inoue T, Shimada H, Kojim S. The mechanisms of nickel uptake by rat primary hepatocyte cultures: role of calcium channels. *Toxicology* 1997;124:21–6.

[35] Lobo AO, Antunes EF, Machado AHA, Pacheco-Soares C, Travai-Airoldi VJ, Corat EJ. Cell viability and adhesion on as grown multi-wall carbon nanotube films. *Mater Sci Eng C* 2008;28:264–9.

[36] Bogdanski D, Koller M, Muller D, Muhr G, Bram M, Buchkremer HP, et al. Easy assessment of the biocompatibility of Ni-Ti alloys by *in vitro* cell culture

experiments on a functionally graded Ni–NiTi–Ti material. *Biomaterials* 2002;23:4549–55.

[37] Ryhanen J, Kallioinen M, Tuukkanen J, Junila J, Niemela E, Sandvik P, et al. *In vivo* biocompatibility evaluation of nickel-titanium shape memory metal alloy: muscle and perineural tissue responses and encapsule membrane thickness. *J Biomed Mater Res* 1998;41:481–8.

[38] Poon RWY, Yeung KWK, Liu XY, Chu PK, Chung CY, Lu WW, et al. Carbon plasma immersion ion implantation of nickel-titanium shape memory alloys. *Biomaterials* 2002;26:2265–72.